POLITECNICO DI TORINO
Repository ISTITUZIONALE

A Multivariate Experimental Design to Investigate the Effect of Different Heat Treatment Procedures and Parameters' Interactions on the Hardness and Retained Austenite of K340

Original
A Multivariate Experimental Design to Investigate the Effect of Different Heat Treatment Procedures and Parameters' Interactions on the Hardness and Retained Austenite of K340 Cold-work Tool Steel / Kenevisi, M.S., Biamino, S., Ugues, D.. - In: JOURNAL OF MATERIALS ENGINEERING AND PERFORMANCE. - ISSN 1059-9495. - 34:(2025), pp. 17746-17758. [10.1007/s11665-024-10486-7]

Availability:
This version is available at: 11583/2994883 since: 2024-11-29T15:47:50Z

Publisher:
Springer

Published
DOI:10.1007/s11665-024-10486-7

Terms of use:

This article is made available under terms and conditions as specified in the corresponding bibliographic description in the repository

Publisher copyright
Springer postprint/Author's Accepted Manuscript

This version of the article has been accepted for publication, after peer review (when applicable) and is subject to Springer Nature's AM terms of use, but is not the Version of Record and does not reflect post-acceptance improvements, or any corrections. The Version of Record is available online at: http://dx.doi.org/10.1007/s11665-024-10486-7

(Article begins on next page)

18 November 2026

A Multivariate Experimental Design to Investigate the Effect of Different Heat Treatment Procedures and Parameters' Interactions on the Hardness and Retained Austenite of K340 Cold-work Tool Steel

Mohammad Saleh Kenevisi [1,2,*], Sara Biamino [1,2,3], Daniele Ugues [1,2,3]

[1] Department of Applied Science and Technology (DISAT), Politecnico di Torino, Italy

[2] Integrated Additive Manufacturing iAM@PoliTO Center, Politecnico di Torino, Italy

[3] National Interuniversity Consortium of Materials Science and Technology (INSTM), Italy

* Corresponding author: saleh.kenevisi@polito.it

Abstract

High-carbon, high-chromium cold work tool steels are a group of steels that are used in various industrial applications due to their exceptional properties such as high hardness and wear resistance. Heat treatment plays a critical role in tailoring these characteristics for each application to meet the required needs. This study investigates the effect of austenitizing and tempering temperatures and tempering steps on the hardness and retained austenite (RA) content and aims at providing a model which can estimate the resulting hardness of each heat treatment recipe. Fifteen heat treatment procedures were defined using a face-centered central composite design. The microstructure of the material was studied by scanning electron microscopy (SEM) and energy dispersive spectroscopy (EDS), and the RA was measured by X-ray diffraction. Vickers microhardness measurement was also used to characterize the mechanical properties of the material. The results showed that austenitizing at 1040 °C and 3-step tempering at 550 °C resulted in the minimum hardness value (732HV). However, the maximum hardness (801HV) was achieved when the material was austenitized at 1055 °C and tempered at 525 °C for 3 steps. The data was analyzed by Chemometric Agile Tool (CAT) software and the results showed that the interaction of austenitizing and tempering temperatures had the most significant effect on hardness. On the other side, the amount of RA was mainly affected by the tempering temperature. By increasing the austenitizing temperature from 1040 to 1070 °C, an increase in the peak hardness value was observed. Additionally, by increasing the tempering

temperature the hardness increased followed by a decline after reaching a peak value. Given the generated model, this research contributes to a deeper understanding of intricate relationships between heat treatment parameters and material properties, facilitating the design of heat treatment procedures based on requirements of each specific application.

Keywords: *Cold-work; Tool steel; Heat treatment; Hardness; Retained Austenite*

1. Introduction

K340 is a type of cold-work tool steel that primarily contains chromium, molybdenum, vanadium, and niobium as alloying elements. It has a remarkable combination of properties, including outstanding resistance to wear, toughness, ultimate strength, and dimensional stability. This alloy is widely utilized in many applications such as construction machinery components, wear-resistant structural parts, stamping and forming dies, blanking and shearing tools, cold heading and extrusion dies, and precision tools [1]. Due to its exceptional wear resistance, it is highly suitable for use in applications that include abrasive wear and high-stress loads. However, stamping tool made of high Cr content cold work too steels are prone to cracking, chipping, and breakage due to the segregation of the alloying elements and the presence of large primary carbides in the microstructure [2].

The microstructure of cold work tool steels is characterized by the presence of carbides that are dispersed in the matrix. The high concentration of alloying elements in these steels leads to the segregation of these elements during the solidification process, resulting in the formation of primary carbides, such as MC, M_2C, and M_7C_3, which remain mainly undissolved even at austenitizing temperature [3]. Additionally, secondary carbides, such as $M_{23}C_6$, form during the hardening heat-treatment process. This attribute greatly enhances the steel performance, particularly under demanding conditions. In tool steels, reducing the amounts of C and Cr results in a decrease in the hardness of the martensite after quenching and the size of secondary carbides. On the other hand,

higher levels of Mo and V improve the hardenability [4]. Generally, the type, size, and the distribution of these carbides play a significant role in the performance and lifetime of tool steels [5].

However, the mechanical properties of the alloy can be highly affected by the heat treatment procedure which modifies the microstructure of the material [6,7]. Research has demonstrated that post-heat treatment procedures can enhance the characteristics of tool steels, suggesting that heat treatment can enhance wear resistance and tailor properties for specific applications [8,9]. This steel is categorized as an air-hardening, high-carbon, high-chromium tool steel. It is subjected to specific heat treatment procedures to attain the desired level of hardness and toughness required for its intended purpose. The heat treatment process for tool steels typically consists of three primary stages: austenitizing, quenching, and tempering [10]. Austenitizing promotes the dissolution of carbides in the matrix and quenching at high cooling rates facilitates the formation of desired phases, such as martensite. Tempering step stimulates the precipitation of small carbides in the martensitic matrix, which are known as secondary carbides. If the quenching is performed at high cooling rates, the risks of cracks and distortion is increased. This risk can be reduced by austempering treatment; however, low fracture and impact toughness can be achieved [11]. Pierer et al. [12] noted that quenching medium can affect the dimensional stability of the parts. Dimensional stability after heat treatment is vital to ensuring the precision, durability, and functionality of industrial components. Their study on K360 alloy showed that the minimum dimensional change was introduced by oil quenching, while salt bath quenching shows a lower degree of change, and the smallest dimensional change occurs with gas quenching. They also claimed that dimensional change increases by increasing the austenitizing temperature.

The mechanical behavior, such as wear properties, hardness, and fracture toughness, of tool steels in relation to austenitizing temperature and tempering conditions has also been the subject of research [13,14]. Bandriyana et al. [15] investigated the impact of heat treatment on the microstructure of an oxide dispersion-strengthened steel. Their research reveals how austenitizing and tempering

processes affect the material's characteristics. For instance, austenitizing temperatures should be carefully chosen to avoid coarsening of prior austenite grains and poor steel toughness [16].

Retained austenite (RA) is commonly found in as-quenched tool steels, especially in steels with high carbon content or certain alloying elements. Its presence can affect the mechanical properties and dimensional stability of the material, so post-quenching treatments like tempering or cryogenic processing are often employed to control or reduce it [17–19].

Regarding the effect of heat treatment on hardness of the material, Feuerhahn et al. [20] processed a tool steel with a chemical composition comparable to K340 by selective laser powder bed fusion (PBF-LB) technique and the hardness of the material was increased from 493 HV to 765 HV after austenitizing the as-built sample at 1080 °C and performing 3-step tempering at 535 °C, to maximize the intensity of carbides precipitation. The effect of austenitizing temperature on the fraction of primary carbides was studied and it was reported that for a D3 tool steel, by increasing the austenitizing temperature from 850 to 1050 °C the volume percentage of chromium carbide was reduced from 8.7% to 4.1% [21].

The latest progress in the enhancement of K340 tool steel has been centered around optimizing its mechanical properties, machinability, and thermal stability. Advanced heat treatment techniques and alloy adjustments have led to improved performance and prolonged lifespan of tools. Furthermore, the progress in surface treatments and coatings has broadened the scope of uses for K340 tool steel. The wear of tools and dies are a major concern in metal forming processes such as blanking and stamping, because of the maintenance costs, the stoppage in the production line, and material wastage as scraps. Due to the high levels of stress applied to the tools, the wear properties of the material are of great importance [22]. The wear resistance of steels is often enhanced by the martensitic phase transformation by applying heat treatment procedures [23]. Applying nitride coatings by physical vapor deposition (PVD) process is a new trend to enhance tribological performance and mitigate the degradation of cold work tools [24,25]. It is also shown that wear properties are dominantly affected

by hardness, which itself is affected by the microstructure [26,27]. Thus, to minimize the extent of tool wear during stamping, it is important to fully understand the parameters that influence these characteristics to effectively prolong the lifespan of the die materials.

Mitigation of sudden die failure is frequently linked to a crucial threshold of hardness that should not be surpassed for a given application. For many applications, the impact of ductility on die longevity surpasses that of toughness, and hardness exhibits a close correlation with both ductility and toughness [28]. Since the hardness of tool steels can be modified by heat treatment, a not optimized heat treatment for each specific application can reduce the service life of the component and result in an early failure. Moreover, one specific material may be used for different applications which require different mechanical properties. This highlights the criticality of optimizing heat treatment procedures to attain the intended microstructures and properties for the service requirements.

Therefore, the main aim of this study is to find a model that can demonstrate the correlation between heat treatment parameters (austenitizing and tempering temperatures and tempering steps) and the resulting hardness value and RA of K340 steel. As a result, by having this model and based on the service requirements, a proper heat treatment procedure can be designed and applied to achieve the desired hardness for the component at a given service condition.

2. Experimental Procedure

The material used in this study was Böhler K340 Isodur cold work tool steel provided by Util Industries S.p.A. The chemical composition of the alloy was analyzed by optical emission spectroscopy technique using Metal LAB Plus equipment produced by GNR s.r.l. and the results are presented in Table 1.

Table 1 – Chemical composition (wt.%) of the alloy used in this study.

Element	C	Cr	Mo	V	Si	Mn	Al	Nb

Avg. measured	0.92	7.98	2.05	0.45	0.71	0.38	0.92	0.11
Nominal	1.1	8.3	2.1	0.5	0.9	0.4	+	+

To define the experiments, the design of experiment (DoE) method using a face-centered central composite design was used. A face-centered central composite design (FCCD) is a type of response surface methodology used to optimize experimental conditions. It consists of factorial points, axial points located on the faces of the factorial space, and center points, which allows for efficient exploration of quadratic relationships. The heat treatment parameters studied in this work were austenitizing and tempering temperatures and tempering steps. For each parameter three levels (-1: minimum, 0: mid-range, and 1: maximum) were defined. The minimum, mid-range, and maximum values for the austenitizing temperature were 1040, 1055, and 1070 °C and it was 500, 525, and 550 °C for the tempering temperature, respectively. Additionally, 1, 2 and 3 steps of tempering, each for one hour, were different levels of tempering. These ranges were selected based on a comprehensive review of relevant literature and the recommendations provided by the alloy manufacturer. Specifically, these parameters were determined to meet the industrial application requirements of the alloy, in order to cover the desired hardness values within the specified limits for such applications. To increase the accuracy of the model at the center point, two replicates were also performed at the center point of the design cube, where all the three parameters have a level of 0, and the reported result for this condition is the average of the three values. Therefore, the following 15 experiments were defined, as provided in Table 2.

Table 2 – Details of the designed experiments.

No.	Austenitizing temp (°C)	Tempering temp (°C)	Tempering steps
1	1040	500	1
2	1070	500	1
3	1040	550	1
4	1070	550	1
5	1040	500	3
6	1070	500	3
7	1040	550	3

8	1070	550	3
9	1040	525	2
10	1070	525	2
11	1055	500	2
12	1055	550	2
13	1055	525	1
14	1055	525	3
15	1055	525	2

Specimens of 10 × 10 × 10 mm^3 were prepared and the heat treatments were carried out at different conditions using Nabertherm LH 60/14 furnace. The holding time for austenitizing was 30 minutes for all conditions. Samples were oil quenched after austenitizing and tempered for different times, each time for one hour, followed by air cooling. The heat treatment procedures are schematically illustrated in Figure 1.

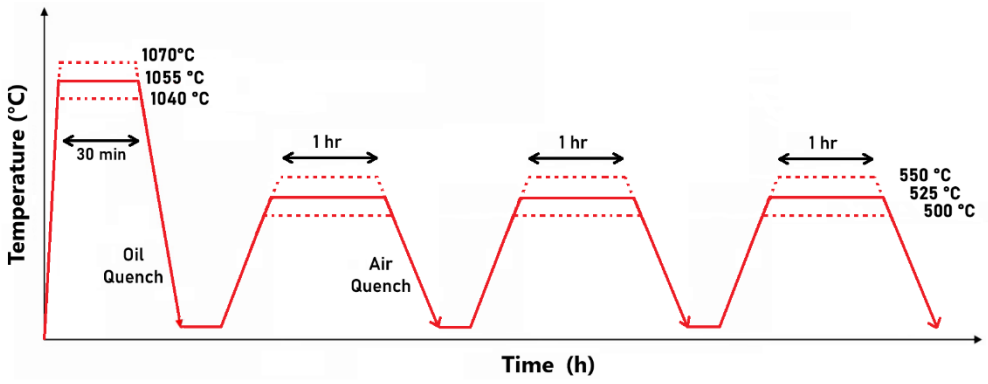


Figure 1 – Schematic illustration of the heat treatment recipes.

Samples were then cut and grinded by SiC papers with different grit sizes. The final polishing was done by 0.25 µm diamond suspension, and Nital 3% was used as the etching solution.

Microstructural analysis was performed by Zeiss EVO 15 scanning electron microscope (SEM) equipped with Ultim Max EDS detector by Oxford Instruments. Thermodynamic simulations were also performed by JMatPro software. Microhardness of the samples were measured by a VMHT 1200 Leica micro-Vickers hardness tester by applying 500 g force with a dwell time of 15 s. The volume fraction of RA was measured by X-ray diffraction, using Pulstec µ-X360s equipment with Cr cathode. After directing X-rays onto the material's surface, the diffraction patterns are collected and analyzed

to determine the presence and quantity of specific phases, such as austenite and martensite. The proportion of RA is then calculated by evaluating the relative intensities of the austenite peaks compared to those of the other phases. The measurement was performed at three different locations for each sample and the average value was reported.

The response surfaces and the effect of different heat treatment parameters on the hardness and RA of the material were prepared and analyzed by Chemometric Agile Tool (CAT) software based on R, a programming language for statistical computing.

3. Results and Discussion

3.1. Microstructural Analysis

Generally, the microstructure of the samples is characterized by the presence of primary and secondary carbides within the martensitic matrix. However, austenitizing at higher temperatures can lead to an increase in the grain size. The preliminary investigations, based on the intercept method, showed that the average austenite grain size was about 11.3 ± 0.2 µm for samples that were austenitized up to 1055 °C. By austenitizing at 1070 °C, the value increased to 12.2 ± 0.3 µm.

The microstructure of the sample which is austenitized at 1040 °C and tempered at 550 °C for 3 steps is provided for reference, as shown in Figure 2.

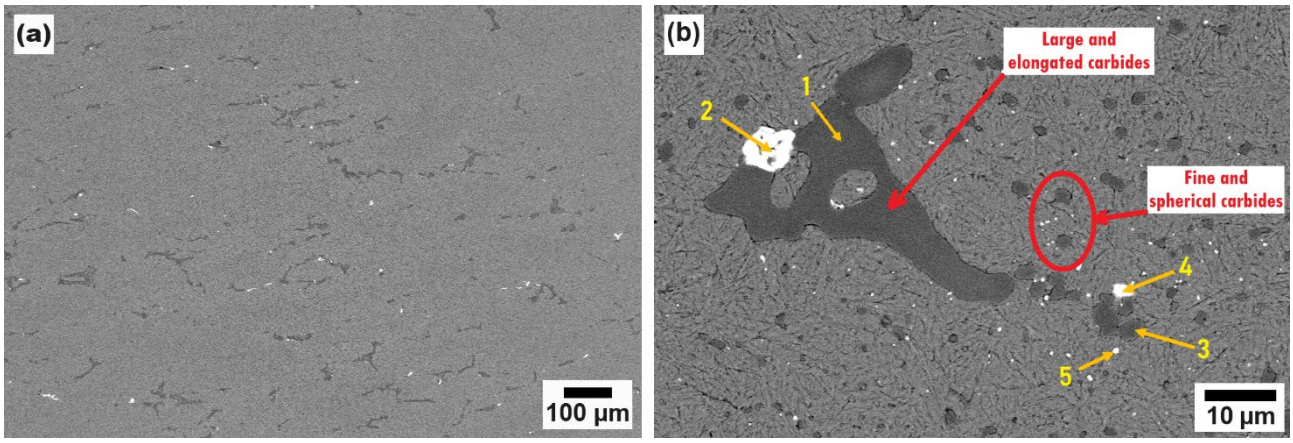


Figure 2 – SEM micrographs of sample 7 (austenitized at 1040 °C and tempered for 3 steps at 550 °C) at different magnifications.

As it can be observed, both relatively large and elongated primary carbides and fine and close to spherical secondary carbides are present in the matrix. Table 3 provides the composition of these carbides obtained by EDS analysis.

Table 3 – EDS analysis results (at.%) of the carbides found in the microstructure.

Location	Al	V	Cr	Mn	Fe	Nb	Mo
1	0.08	6.14	47.88	0.50	39.89	0.13	5.38
2	0.73	7.71	5.35	0.14	30.47	46.13	9.49
3	0.26	4.89	46.69	0.43	43.11	0.07	4.54
4	1.57	2.29	8.78	0.42	68.71	13.24	4.99
5	2.26	0.25	6.86	0.64	88.37	0.02	1.60

In addition to Table 3, the EDS mapping, presented in Figure 3, shows that the big bright regions are Nb carbides with some Mo contents. Additionally, the dark grey carbides are rich in Cr, V, Mo, and Mn. Secondary carbides are precipitated during the tempering step as a consequence of a diffusive transformation [29].

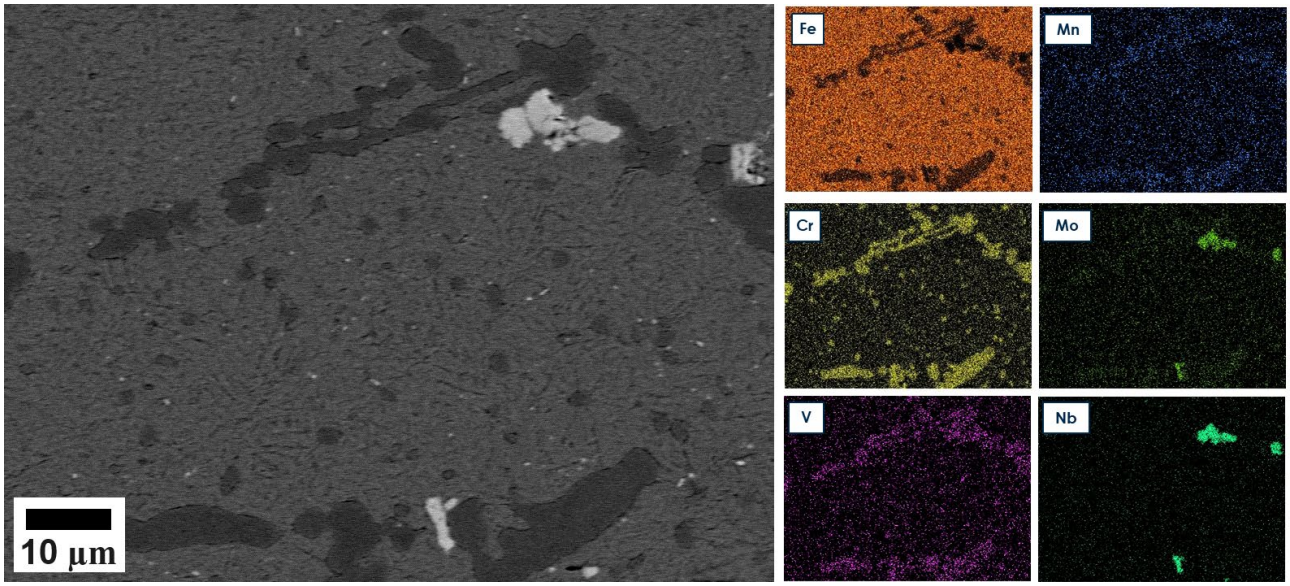


Figure 3 – EDS map of a region of sample #7.

Although sample was austenitised, the primary carbides did not fully dissolve into the matrix, as the dissolution of primary carbides occurs at temperatures higher than around 1150 °C [30,31]. It is reported that MC (rich in V and Nb), M_6C (rich in Cr, Mo, and V), M_7C_3, and $M_{23}C_6$ (all rich in Cr and Fe) can be found in the microstructure of quenched tempered K340 alloy [17,32].

Thermodynamic simulation made by JMatPro, Figure 4, also confirms the presence of these carbide in the microstructure.

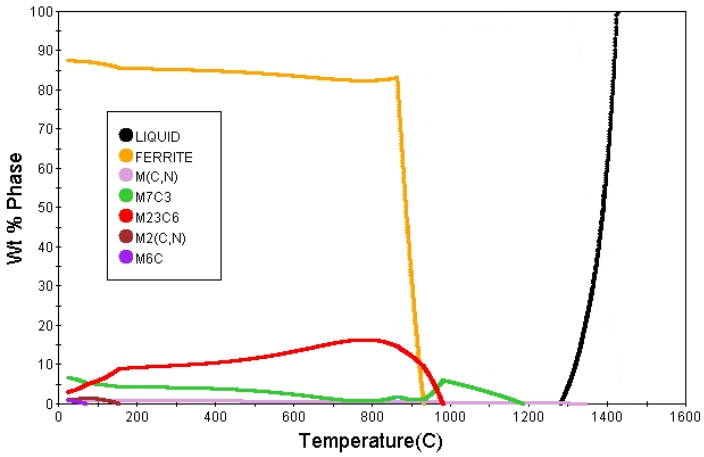


Figure 4 – Thermodynamic properties calculation of the alloy used in the study with the measured chemical composition.

3.2. Hardness Measurement

Microhardness measurements were done at five different locations for each sample and the average values are reported in Table 4.

Table 4 – Microhardness values (HV) obtained for samples heat treated at different conditions.

Sample	1	2	3	4	5	6	7	8	9	10	11	12	13	14	15
Hardness	759.5 ±4.7	744.6 ±6.1	777.2 ±4.8	790.3 ±3.6	783.1 ±5.3	776.0 ±4.8	731.9 ±2.3	795.1 ±2.6	765.9 ±4.5	794.3 ±4.2	760.0 ±3.5	775.2 ±6.4	778.9 ±5.8	801.1 ±6.0	783.7 ±4.5

The results showed that the hardness values varied between around 745 to 801 HV. To have a general overview on how the combined time and temperature of tempering can affect the hardness of the material, the Larson Miller Parameter (LMP) was used, which describes how the hardness is affected by the heat treatment procedure. LMP is defined in Eq.1 as follows [33]:

$$LMP = T \times [20 + log(h)] \times 0.001 \qquad \textit{Equation 1}$$

where T is the tempering temperature in [K] and h is the tempering time in hour. It is a very useful way to illustrate the effects of temperature and time on the material properties during heat treatment. The LMP combines time and temperature into a single parameter, allowing for the estimation of how heat treatment impacts the microstructure and mechanical properties such as

hardness, and ensuring more accurate predictions of material behavior under specific heat treatment conditions. It can be claimed that increasing tempering time and temperature should result in higher values of LMP. The LMP was calculated for samples austenitized at different temperatures, and was plotted versus the hardness, as shown in Figure 5.

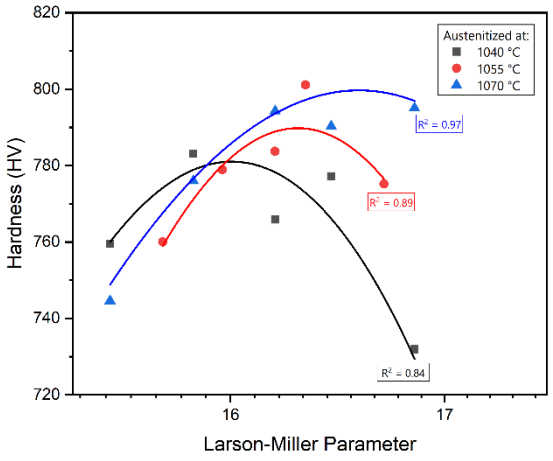


Figure 5 – Plot of LMP against hardness at different austenitizing temperatures.

According to Figure 5, for all austenitizing temperatures, by increasing the LMP, the hardness tends to increase to reach a peak value, followed by a decrease. The initial raise can be attributed to the precipitation of secondary carbides and the occurrence of RA to martensite transformation. On the other side, the following reduction can be the result of the formation of coarser precipitates occurring at higher temperatures and of the softening of the martensitic phase. Coarsening happens when smaller carbides start to dissolve in the matrix and their alloying elements diffuse through the matrix to coarsen the larger carbides. The solubility of carbides and the atom mobility of the alloying elements are important factors affecting the coarsening behavior, which is described by Ostwald ripening model [34]. Precipitates with a longer average distance between them contribute less to the hardening [35]. A similar trend was observed by Farahany et al. [32] and Lin et al. [36] by increasing the tempering temperature of K340 and 0.63C-12.7Cr steels, respectively. Carbide coalescence can occur when adjacent carbide particles merge to form a larger particle. This process is facilitated by atomic diffusion at the carbide-carbide interface. Additionally, at high temperatures, atoms of

carbide-forming elements (such as carbon, chromium, molybdenum, and vanadium) diffuse through the matrix and further contribute to the growth of carbides [37].

The hardness drop is more severe when the material is austenitized at 1040 °C compared to other austenitizing temperatures. Generally, when the material is austenitized at higher temperatures, more RA would remain after quenching, which can be transformed to martensite after tempering. Therefore, when the material is austenitized at higher temperatures the reduction in hardness (by increasing tempering temperature and time) can be compensated more by having more austenite to martensite transformation. Additionally, in the sample austenitized at a lower temperature, the initial martensitic structure contains fewer alloying elements that strengthen the material during tempering. These make the material more prone to significant softening during extended tempering, leading to a more severe drop in hardness.

In general, austenitizing at higher temperatures led to higher peak hardness values. The same result was observed by Rehan et al. [2] when 5 wt.% Cr cold work tool steel was austenitized at different temperatures. This can be discussed by the fact that more of alloying elements can diffuse into the austenite and a more uniform distribution of alloying elements and carbides can be obtained. In other words, the dissolution of primary carbides, such as M_7C_3, during austenitization introduces alloying elements into the matrix. As a result, higher austenitization temperatures lead to the formation of greater amounts of tempering carbides, which significantly contribute to the peak of secondary hardening.

3.3. Surface Responses and Analysis

By using the CAT software, the effect of three variables on the material's hardness can be systematically investigated. Additionally, a model can be created which makes it possible to predict the resulting hardness for any heat treatment procedure when the values of the parameters are selected between the minimum and maximum corresponding values chosen in this work.

As depicted in Figure 6a, the austenitizing temperature had the most significant effect on the hardness, followed by tempering temperature. Tempering step was also the variable which had the least effect compared to the other two factors. Concerning the model calculations and its effectiveness (Figure 4b), it can be seen that the created model was relatively accurate as the predicted values are close to the experimental ones having an $R^2 = 0.90$.

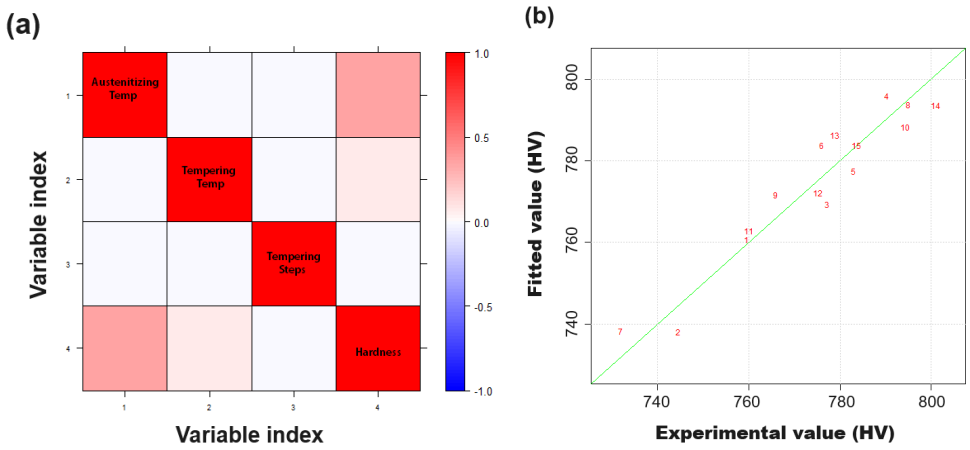


Figure 6 – Plots showing a) the correlation of hardness with different variables and b) the goodness of fit of the model.

To have in-depth analysis of the correlation between the variables and the yield, surface responses were plotted for different conditions. As austenitizing and tempering temperatures were the two main affecting parameters, the effect of these two variables on hardness value at different tempering steps was plotted and is illustrated in Figure 7.

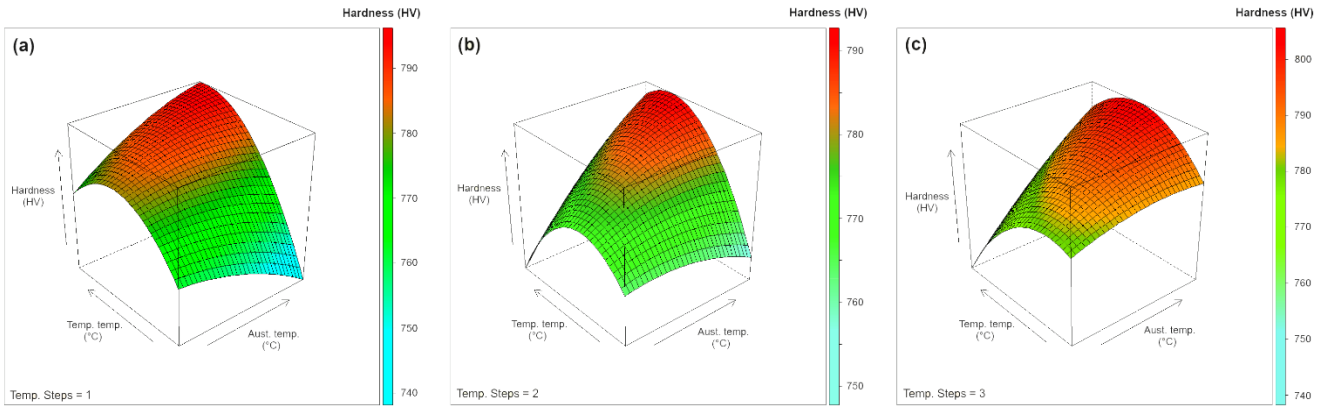


Figure 7 – Response surfaces showing the effect of austenitizing and tempering temperatures on hardness value when the material is tempered for a) 1 step, b) 2 steps, and c) 3 steps.

Comparing the graphs reveals that by increasing the tempering steps the maximum hardness achieved has increased. As discussed earlier, this is due to the completion of martensitic transformation and carbides precipitation. Furthermore, the impact of tempering temperature on hardness is more significant when the material is austenitized at higher temperatures compared to when it is austenitized at lower temperatures. Likewise, the effect of austenitizing temperature is not that significant when the material is tempered at low temperatures close to 500 °C. Interestingly, the hardness value tends to decrease by increasing the austenitizing temperature when the material is tempered for just one step at 500 °C. The results suggest that secondary hardening is not activated at low tempering temperatures and times, and descending in the hardness can be mainly attributed to the increased content of RA in the microstructure of the material austenitized at elevated temperatures. Additionally, grain coarsening of the austenite at higher temperatures can play a role as well. The results showed that the peak of secondary hardening occurred at around 525 °C when the material is austenitized at 1070 °C. When the material is tempered at 500 – 525 °C, the precipitation of nano-sized carbides within the matrix increases the hardness. However, by increasing the tempering temperature, these carbides coarsen and exert a lower impact on hardening of the material. The secondary hardening is reported to start at 500 °C for D3 tool steel [21].

In all cases, the maximum hardness is achieved when the material is austenitized at 1070 °C. Austenitizing at higher temperatures leads to an increased dissolution intensity of primary carbides, such as M_7C_3, and provides an austenite with more alloying elements available [2]. Therefore, more secondary carbides are precipitated during the tempering, which provides a higher hardening peak. These secondary carbides are contributing more to the hardening as they are coherent, fine, and uniformly distributed in the microstructure.

Tempering of medium and high carbon steels at different temperatures results in the precipitation of different carbides. It is reported that when these steels are tempered below 200 °C the precipitation of ε carbides occurs [16]. By tempering within the ranges of 200 – 350 °C and 500 – 600 °C, M_3C

and MC/M_2C carbides will form, respectively [6,38]. It is also reported that tempering temperature can affect the size of the carbides [39]. Therefore, the diminution of hardness by increasing the tempering temperature can be due to the increase in the carbides size, which was discussed earlier in section 3.1. Matrix softening was also observed when the tempering temperature of a 42CrMo4V alloy was increased from 570 to 720 °C [40].

The DoE contour plot is commonly used to identify optimal settings that will either maximize or minimize the response variable. Figure 8 shows contour plots at different heat treatment procedures.

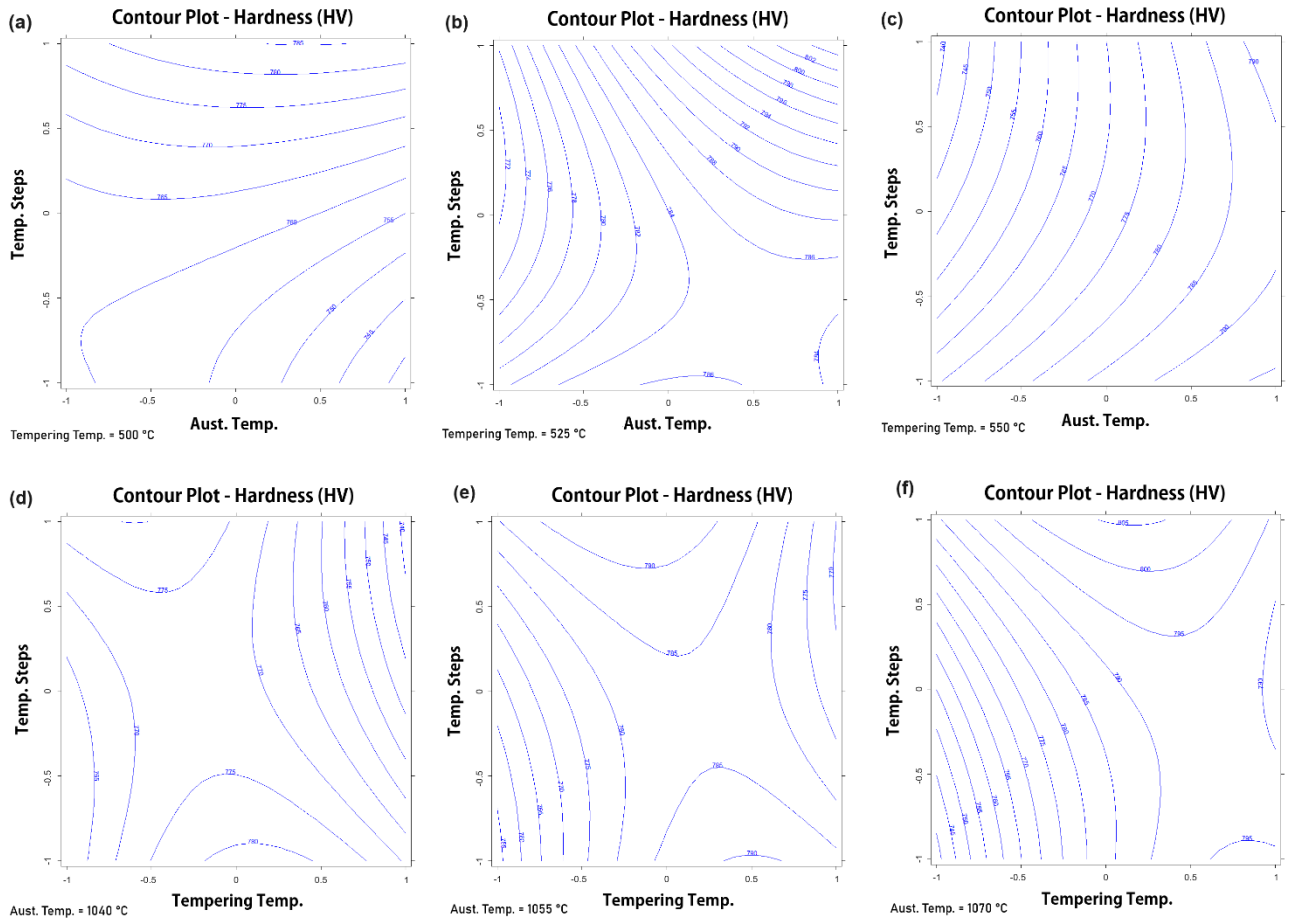


Figure 8 – Contour plots illustrating the correlation of austenitizing temperature, tempering steps, and hardness at tempering temperatures of a) 500, b) 525, c) 550 °C and the correlation of tempering temperature and steps and hardness at austenitizing temperatures of d) 1040, e) 1055, and f) 1070 °C.

Generally, a denser concentration of contour lines indicates a steeper gradient, showing that the response is highly sensitive to changes in the factors in that region. Therefore, comparing Figure 8a and b, it can be concluded that at a tempering temperature of 525 °C the hardness is more sensitive

to the changes in the austenitizing temperature. The contour plots can also assist in identifying sets of processing parameters that lead to the response variable reaching a predetermined target value. As an example, according to Figure 8d, it can be seen that there is a range of tempering temperatures and tempering steps that can be chosen expecting no change in the hardness value.

Based on the experimental results, statistical analysis, and the interactions between the variables (austenitizing temperature, and tempering temperature and steps) the following model (Eq. 2) can be generated:

$$H = 783.91 + 8.27\,X_1 + 4.56\,X_2 + 3.67\,X_3 + 12.29\,X_1X_2 + 7.24\,X_1X_3 - 11.94\,X_2X_3 - 3.86\,X_1^2 - 16.36\,X_2^2 - 6.04\,X_3^2 \quad \textit{Equation 2}$$

Where H is the hardness value in HV, X_1 is austenitizing temperature, X_2 is tempering temperature, and X_3 is tempering steps. By using this model, with an acceptable accuracy, the hardness can be estimated when any heat treatment procedure is applied within the defined range of the model (austenitizing temperature: 1040-1070 °C, tempering temperature: 500-550 °C, and tempering steps: 1-3). However, it is worth noting that all X_n values shall be first converted into -1 to 1 scale and then replaced in equation 2 for hardness prediction.

3.4. Retained Austenite Analysis

In high alloy steels, the resulting microstructure after quenching from the austenitizing temperature generally consists of martensite, carbides, and RA. According to the continuous cooling transformation (CCT) diagrams plotted by JMatPro and given in Figure 9, with a high cooling rate provided by oil quenching, the austenite transforms to martensite. However, having a martensite start (M_s) temperature around 150 °C and a martensite finish (M_f) below the room temperature, some RA will remain in the microstructure.

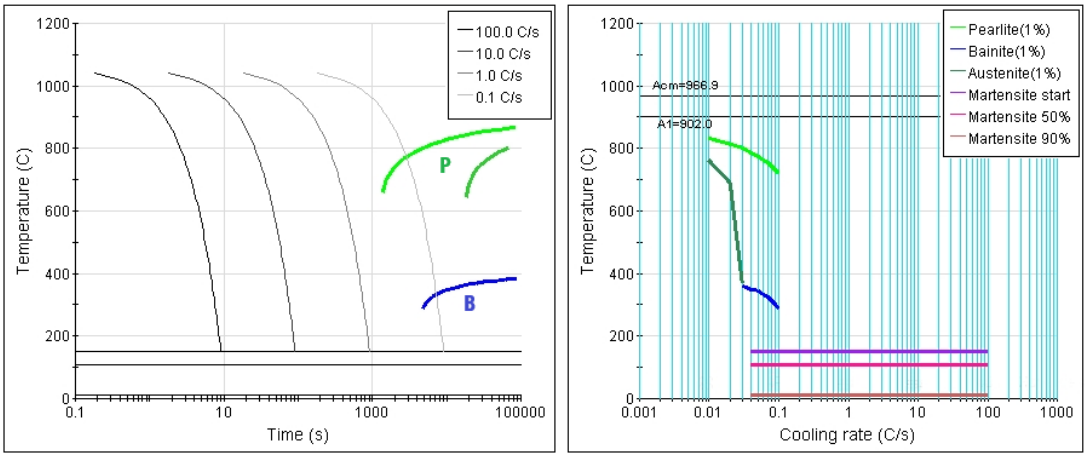


Figure 9 – CCT diagrams of the alloy plotted by JMatPro.

It is stated that segregation of the alloying elements at grain boundaries or at interdendritic regions further decreases the M_s temperature leading to the presence of RA in the microstructure [41]. The RA is normally visible as brighter regions in an etched cross-section, as shown in Figure 10.

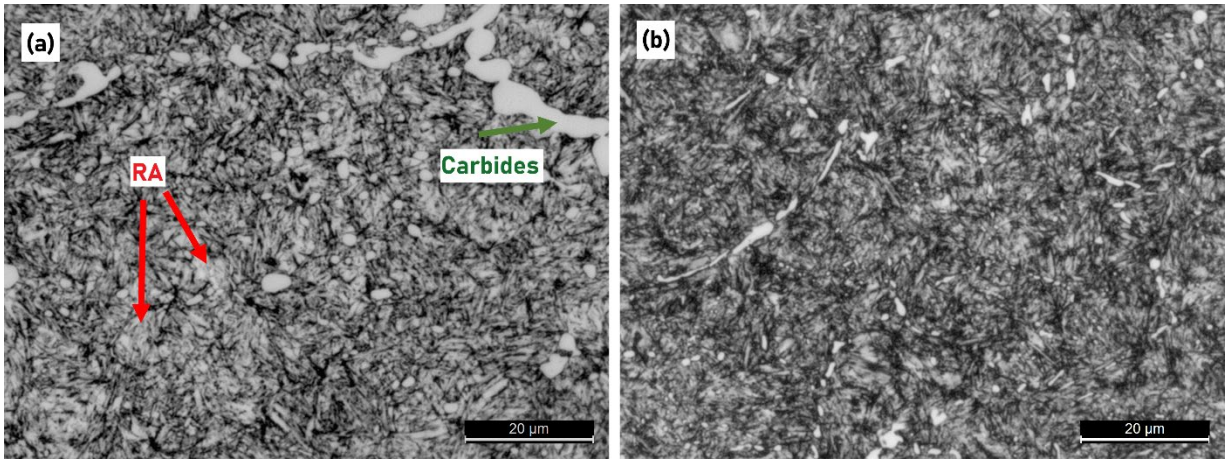


Figure 10 – LOM micrographs showing the RA in the microstructure of samples a) 6 (high amount of RA) and b)7 (with low amount of RA).

It should be noted that some of the RA can be transformed to martensite during the polishing stage, which can reduce the RA amount detectable by optical microscopy [42,43]. RA can influence the mechanical properties of the material, such as hardness which is of interest in this study. The RA of each sample was measured, and the results are provided in Table 5, and the debye rings and phase-related peaks of two samples with low and high RA is presented in Figure 11.

Table 5 – The fraction of RA (in %) in the microstructure of the heat-treated samples.

Sample	1	2	3	4	5	6	7	8	9	10	11	12	13	14	15
R.A.	12.8 ± 0.2	20.8 ± 0.6	3.5 ± 0.4	10.2 ± 0.5	13.9 ± 0.1	21.0 ± 0.1	1.3 ± 0.1	2.5 ± 0.4	10.0 ± 0.3	16.5 ± 0.2	19.0 ± 0.3	2.5 ± 0.2	16.9 ± 0.1	10.4 ± 0.1	13.2 ± 0.6

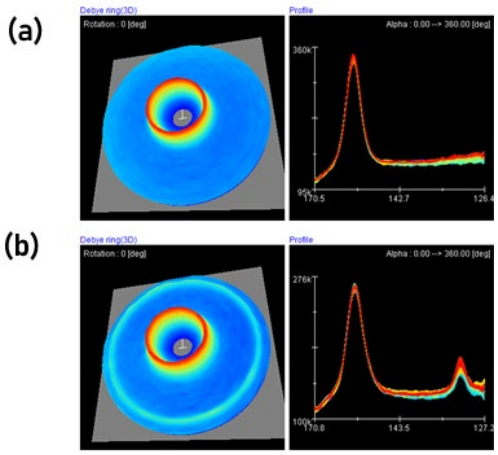


Figure 11 – Representative XRD results of samples a) 7 with low RA and b) 13 with relatively high RA content.

It can be observed that the RA in the samples that are tempered at higher temperatures is generally lower than that of the others. Higher tempering temperature causes the RA phase to undergo a transformation to other phases, like martensite, upon cooling [44]. This transformation is driven by the thermodynamics of the system, where higher temperatures provide enough energy to overcome the stability of RA, causing it to decompose. This is also facilitated by increased carbon diffusion out of the austenite, which leads to the precipitation of carbides and further destabilizes the RA. Additionally, by comparing samples 9, 10, and 15, it can be concluded that increasing the austenitizing temperature increases the amount of RA. To obtain more in-depth information about how the three HT parameters can affect the RA, a new model was generated, and statistical analysis was performed on the data. Figure 11a represents the residuals in fitting, which is the difference between the experimental and fitted values. Generally, a good model should have residuals that are small and randomly distributed, indicating that the model's predictions closely match the observed values. The results showed that the residuals are within the range of about ±1.7, which suggests a good fitting. Additionally, R^2 was measured to be 0.97, which also confirms the accuracy of the regression model. Figure 11b illustrates how each factor and a combination of them contribute to

the change in RA. The sign of a coefficient (positive or negative) indicates the direction and nature of the relationship between factor and response, and the magnitude (absolute value) of a coefficient reflects the strength of the effect the factor has on the response. Therefore, it can be concluded that tempering temperature is the most significant factor affecting the content of RA in the microstructure. Austenitizing temperature and tempering temperature squared are the next most-affecting parameters. It can also be concluded that the amount of RA increases by increasing the austenitizing temperature. However, increasing the tempering temperature or steps can lead to lower fractions of RA.

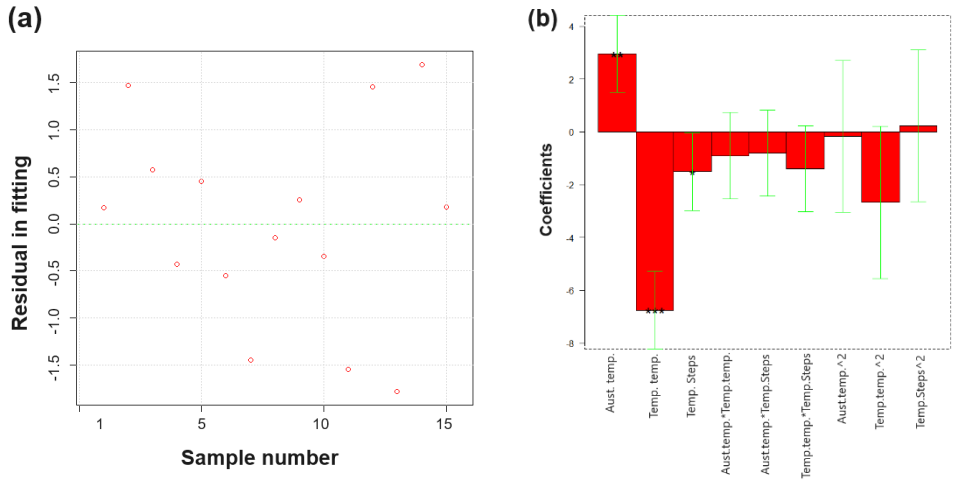


Figure 12 – a) Residuals in fitting (difference between the experimented and predicted values) and b) representation of the significance of each HT parameter on the content of RA.

Austenitizing at higher temperatures results in a higher fraction of RA in the microstructure after quenching as a result of lower martensite start and finish temperatures. During the process of austenitizing, the primary carbides undergo partial dissolution, resulting in an increase in the concentration of alloying elements in the austenitic matrix. Increasing the alloy content in the austenite reduces the temperature at which the martensite transformation begins (M_s) and ends (M_f) during the quenching process [2]. For certain types of steels, these temperatures may be significantly higher than room temperature, leading to the development of a microstructure that is entirely martensitic. However, in the case of medium and high alloyed steels, it is typical for the M_f temperature to be lower than the ambient room temperature. Hence, substantial quantities of residual

austenite are present in the microstructure after quenching, especially when the material austenitized at relatively high temperatures.

Tempering the material initiates the precipitation of carbides. This reduces the carbon content of the RA and according to the literature, the transformation of RA to ferrite and cementite, martensite, or bainite occurs by tempering [16,44,45]. The transformation to ferrite and cementite happens isothermally when the material is kept at the tempering temperature, and martensite or bainite can form during cooling down from tempering temperature to room temperature. When there is a high amount of RA in the microstructure, this transformation cannot be completed by a single tempering step. Hence, it is necessary to subject the material to double or occasionally triple tempering treatments to completely transform the RA. Additionally, tempering for longer times increases M_s [30].

The RA content in the microstructure of this alloy is important. The RA is a relatively soft phase which shortens the lifespan of the material when used as a tool. Additionally, this phase can be later transformed into untempered martensite, which is fragile and micro-cracks can develop easily, and affects the dimensional stability of the part [22,46,47]. Therefore, based on the requirements of the material for each specific application, it is essential to control the volume fraction of the RA.

4. Conclusion

In this work, by using a face-centered central composite design, the effect of austenitizing and tempering temperatures and tempering steps on the resulting hardness and RA fraction of K340 cold work tool steel was studied. It can be concluded that:

1. Different heat treatment procedures resulted in a change in the hardness value, which ranged from 732 to 801 HV. Austenitizing at 1040 °C and 3-step tempering at 550 °C resulted in the minimum hardness value. However, the maximum hardness was achieved when the material was austenitized at 1055 °C and tempered at 525 °C for 3 steps.

2. The austenitizing temperature had the greatest influence on hardness, followed by the tempering temperature. Among the three factors, the tempering step had the least impact. The results indicated that higher austenitizing temperatures led to a higher peak in hardness values. Additionally, increasing the number of tempering steps resulted in a further increase in the maximum hardness achieved.
3. Hardness values increased with rising tempering temperatures up to a peak, attributed to the precipitation of secondary carbides and the transformation of RA. Beyond this point, further increases in tempering temperature resulted in a decrease in hardness. However, it is important to note that factors beyond carbide behavior and martensitic transformation, such as grain size, can also play a role in the resulting hardness.
4. Austenitizing at high and tempering at low temperatures resulted in about 21% of RA in the microstructure. Almost no trace of RA was found when the material was austenitized at 1040 °C and tempered at 550 °C for three steps. Austenitizing and tempering temperatures had a direct and inverse relationship with the fraction of RA, respectively. Additionally, having more steps of tempering led to lower amounts of RA in the microstructure.

In summary, this work by providing a model which can estimate the hardness and retained austenite of the material heat treated with different procedures facilitates designing new heat treatment recipes based on the mechanical properties' requirements.

Conflict of Interest: On behalf of all authors, the corresponding author states that there is no conflict of interest.

References

[1] voestalpine BÖHLER Edelstahl GmbH & Co., Cold Work Tool Steel BÖHLER K340, 2020. www.voestalpine.com/bohler-edelstahl.

[2] M.A. Rehan, A. Medvedeva, B. Högman, L.-E. Svensson, L. Karlsson, Effect of Austenitization and Tempering on the Microstructure and Mechanical Properties of a 5 wt% Cr Cold Work Tool Steel, Steel Res Int 87 (2016) 1609–1618. https://doi.org/https://doi.org/10.1002/srin.201600012.

[3] H. Kim, J.Y. Kang, D. Son, T.H. Lee, K.M. Cho, Evolution of carbides in cold-work tool steels, Mater Charact 107 (2015) 376–385. https://doi.org/10.1016/J.MATCHAR.2015.08.001.

[4] K. Fukaura, Y. Yokoyama, D. Yokoi, N. Tsujii, K. Ono, Fatigue of cold-work tool steels: Effect of heat treatment and carbide morphology on fatigue crack formation, life, and fracture surface observations, Metallurgical and Materials Transactions A 35 (2004) 1289–1300. https://doi.org/10.1007/s11661-004-0303-5.

[5] K. Miao, Y. He, N. Zhu, J. Wang, X. Lu, L. Li, Coarsening of carbides during different heat treatment conditions, J Alloys Compd 622 (2015) 513–523. https://doi.org/10.1016/J.JALLCOM.2014.10.115.

[6] G.R. Speich, W.C. Leslie, Tempering of steel, Metallurgical Transactions 3 (1972) 1043–1054. https://doi.org/10.1007/BF02642436.

[7] K. Khatibi, M.B.A. Asmael, B. Safaei, Q. Zeeshan, Solidification and microstructure characterizations of eutectic aluminum-silicon casting alloy with the addition of tin, Materwiss Werksttech 52 (2021) 871–878. https://doi.org/https://doi.org/10.1002/mawe.202100040.

[8] Y.E. Jeong, J.Y. Lee, E.K. Lee, D.S. Shim, Microstructures and Mechanical Properties of Deposited Fe-8Cr-3V-2Mo-2W on SCM420 Substrate Using Directed Energy Deposition and Effect of Post-Heat Treatment, Materials 14 (2021). https://doi.org/10.3390/ma14051231.

[9] E. Bassini, A. Sivo, D. Ugues, Assessment of the Hardening Behavior and Tensile Properties of a Cold-Rolled Bainitic–Ferritic Steel, Materials 14 (2021). https://doi.org/10.3390/ma14216662.

[10] J.L. Dossett, Heat Treatment of Tool Steels, in: Practical Heat Treating: Basic Principles, ASM International, 2020. https://doi.org/10.31399/asm.tb.phtbp.9781627083263.

[11] H. Jesperson, Influence of the heat treatment on the toughness of some hot-work tool steel grades, 2nd Int. Conference Heat Treatment and Surface Engineering in Automotive Applications 98 (2006) 29–37.

[12] R. Pierer, R. Schneider, H. Hiebler, The behaviour of two new tool steels regarding dimension change, in: 6th International Tooling Conference, 2002: pp. 611–624.

[13] V. Jagota, R.K. Sharma, Interpreting H13 steel wear behavior for austenitizing temperature, tempering time and temperature, Journal of the Brazilian Society of Mechanical Sciences and Engineering 40 (2018) 219. https://doi.org/10.1007/s40430-018-1140-6.

[14] V. Leskovšek, B. Šuštaršič, G. Jutriša, The influence of austenitizing and tempering temperature on the hardness and fracture toughness of hot-worked H11 tool steel, J Mater Process Technol 178 (2006) 328–334. https://doi.org/10.1016/J.JMATPROTEC.2006.04.016.

[15] B. Bandriyana, B. Sugeng, R. Salam, D. Hairani, A. Sujatno, N. Shabrina, Effects of heat treatment on the microstructure of the ODS (oxide dispersion strengthened) steel Fe-9Cr-0.5Y2O3, J Phys Conf Ser 2193 (2022) 12046. https://doi.org/10.1088/1742-6596/2193/1/012046.

[16] H.K.D.H. Bhadeshia, Bainite in Steels: Theory and Practice, 3rd Edition, CRC Press, London, 2015. https://doi.org/10.1201/9781315096674.
[17] P. Jovičević-Klug, L. Tóth, B. Podgornik, Comparison of K340 Steel Microstructure and Mechanical Properties Using Shallow and Deep Cryogenic Treatment, Coatings 12 (2022). https://doi.org/10.3390/coatings12091296.
[18] A. Molinari, M. Pellizzari, S. Gialanella, G. Straffelini, K.H. Stiasny, Effect of deep cryogenic treatment on the mechanical properties of tool steels, J Mater Process Technol 118 (2001) 350–355. https://doi.org/10.1016/S0924-0136(01)00973-6.
[19] A. Oppenkowski, S. Weber, W. Theisen, Evaluation of factors influencing deep cryogenic treatment that affect the properties of tool steels, J Mater Process Technol 210 (2010) 1949–1955. https://doi.org/10.1016/J.JMATPROTEC.2010.07.007.
[20] F. Feuerhahn, A. Schulz, T. Seefeld, F. Vollertsen, Microstructure and Properties of Selective Laser Melted High Hardness Tool Steel, Phys Procedia 41 (2013) 843–848. https://doi.org/10.1016/J.PHPRO.2013.03.157.
[21] M. Momeni, S. Kheirandish, H. Saghafian, J. Hedjazi, M. Momeni, Effects of heat treatment on mechanical properties of modified cast AISI D3 tool steel, Materials & Design (1980-2015) 54 (2014) 742–747. https://doi.org/10.1016/J.MATDES.2013.09.002.
[22] M. Muro, G. Artola, A. Gorriño, C. Angulo, Wear and Friction Evaluation of Different Tool Steels for Hot Stamping, Advances in Materials Science and Engineering 2018 (2018) 3296398. https://doi.org/10.1155/2018/3296398.
[23] Y.C. Lin, S.W. Wang, T.M. Chen, A study on the wear behavior of hardened medium carbon steel, J Mater Process Technol 120 (2002) 126–132. https://doi.org/10.1016/S0924-0136(01)01195-5.
[24] S. Kumar, S.R. Maity, L. Patnaik, Friction and tribological behavior of bare nitrided, TiAlN and AlCrN coated MDC-K hot work tool steel, Ceram Int 46 (2020) 17280–17294. https://doi.org/10.1016/J.CERAMINT.2020.04.015.
[25] P. Yan, X. Wang, L. Jiao, Effect of element contents on friction and wear behaviors of ternary nitride coatings, Industrial Lubrication and Tribology 68 (2016) 696–701. https://doi.org/10.1108/ILT-07-2015-0099.
[26] E. Wen, R. Song, W. Xiong, Effect of Tempering Temperature on Microstructures and Wear Behavior of a 500 HB Grade Wear-Resistant Steel, Metals (Basel) 9 (2019). https://doi.org/10.3390/met9010045.
[27] M. Kenevisi, P. Martelli, F. Gobber, D. Ugues, S. Biamino, Processability of K340 Cold Work Tool Steel by Directed Energy Deposition Technique, IOP Conf Ser Mater Sci Eng 1310 (2024) 012021. https://doi.org/10.1088/1757-899X/1310/1/012021.
[28] S. Saha, L. Prasad, V. Kumar, Experimental investigations on heat treatment of cold work tool steels: part 1 , air-hardening grade (D2), Int J Eng Res Appl 2 (2012) 510–519. https://api.semanticscholar.org/CorpusID:17422396.
[29] M. Nurbanasari, P. Tsakiropoulos, E.J. Palmiere, A Study of Carbide Precipitation in a H21 Tool Steel, ISIJ International 54 (2014) 1667–1676. https://doi.org/10.2355/isijinternational.54.1667.
[30] M.A. Rehan, A. Medvedeva, L.-E. Svensson, L. Karlsson, Retained Austenite Transformation during Heat Treatment of a 5 Wt Pct Cr Cold Work Tool Steel, Metallurgical and Materials Transactions A 48 (2017) 5233–5243. https://doi.org/10.1007/s11661-017-4232-5.
[31] H. Jirková, D. Aišman, K. Rubešová, K. Opatová, B. Mašek, Semi-solid processing of high-chromium tool steel to obtain microstructures without carbide network, in: IOP Conf Ser Mater Sci Eng, Institute of Physics Publishing, 2017. https://doi.org/10.1088/1757-899X/179/1/012036.

[32] S. Farahany, M. Ziaie, N.A. Nordin, Effect of Triple Tempering Temperature on Microstructure, Mechanical, and Wear Properties of K340 Cold Work Tool Steel, J Mater Eng Perform 32 (2023) 9000–9010. https://doi.org/10.1007/s11665-022-07791-4.
[33] Y.T. Tang, C. Panwisawas, J.N. Ghoussoub, Y. Gong, J.W.G. Clark, A.A.N. Németh, D.G. McCartney, R.C. Reed, Alloys-by-design: Application to new superalloys for additive manufacturing, Acta Mater 202 (2021) 417–436. https://doi.org/10.1016/J.ACTAMAT.2020.09.023.
[34] K. Miao, Y. He, N. Zhu, J. Wang, X. Lu, L. Li, Coarsening of carbides during different heat treatment conditions, J Alloys Compd 622 (2015) 513–523. https://doi.org/10.1016/J.JALLCOM.2014.10.115.
[35] D.A. Porter, K.E. Easterling, M.Y. Sherif, Phase Transformations in Metals and Alloys, CRC Press, Boca Raton, 2021. https://doi.org/10.1201/9781003011804.
[36] Y. Lin, C.-C. Lin, T.-H. Tsai, H.-J. Lai, Microstructure and Mechanical Properties of 0.63C-12.7Cr Martensitic Stainless Steel during Various Tempering Treatments, Materials and Manufacturing Processes 25 (2010) 246–248. https://doi.org/10.1080/10426910903426307.
[37] S. Yamasaki, Modelling Precipitation of Carbides in Martensitic Steels, University of Cambridge, 2004.
[38] J. Akré, F. Danoix, H. Leitner, P. Auger, The morphology of secondary-hardening carbides in a martensitic steel at the peak hardness by 3DFIM, Ultramicroscopy 109 (2009) 518–523. https://doi.org/10.1016/J.ULTRAMIC.2008.11.010.
[39] A. Kwiatkowski da Silva, G. Inden, A. Kumar, D. Ponge, B. Gault, D. Raabe, Competition between formation of carbides and reversed austenite during tempering of a medium-manganese steel studied by thermodynamic-kinetic simulations and atom probe tomography, Acta Mater 147 (2018) 165–175. https://doi.org/10.1016/J.ACTAMAT.2018.01.022.
[40] C. Sun, P.-X. Fu, H.-W. Liu, H.-H. Liu, N.-Y. Du, Effect of Tempering Temperature on the Low Temperature Impact Toughness of 42CrMo4-V Steel, Metals (Basel) 8 (2018). https://doi.org/10.3390/met8040232.
[41] M.H. Shaeri, H. Saghafian, S.G. Shabestari, Effects of Austempering and Martempering Processes on Amount of Retained Austenite in Cr-Mo Steels (FMU-226) Used in Mill Liner, Journal of Iron and Steel Research, International 17 (2010) 53–58. https://doi.org/10.1016/S1006-706X(10)60059-3.
[42] J. Pechoušek, E. Kuzmann, R. Vondrášek, A. Olina, V. Vrba, L. Kouřil, T. Ingr, P. Král, M. Mashlan, Successive Grinding and Polishing Effect on the Retained Austenite in the Surface of 42CrMo4 Steel, Metals (Basel) 12 (2022). https://doi.org/10.3390/met12010119.
[43] G. Frederic, V. Voort, Metallographic Characterization of the Microstructure of Tool Steels, n.d. https://www.researchgate.net/publication/229048653.
[44] H. Bhadeshia, R. Honeycombe, Steels: Microstructure and Properties, 4th edition, Butterworth-Heinemann, 2017.
[45] A.S. Podder, I. Lonardelli, A. Molinari, H.K.D.H. Bhadeshia, Thermal stability of retained austenite in bainitic steel: an in situ study, Proceedings of the Royal Society A: Mathematical, Physical and Engineering Sciences 467 (2011) 3141–3156. https://doi.org/10.1098/rspa.2011.0212.
[46] O. Barrau, C. Boher, R. Gras, F. Rezai-Aria, Analysis of the friction and wear behaviour of hot work tool steel for forging, Wear 255 (2003) 1444–1454. https://doi.org/10.1016/S0043-1648(03)00280-1.
[47] M.H. Staia, Y. Pérez-Delgado, C. Sanchez, A. Castro, E. Le Bourhis, E.S. Puchi-Cabrera, Hardness properties and high-temperature wear behavior of nitrided AISI D2 tool steel, prior

and after PAPVD coating, Wear 267 (2009) 1452–1461.
https://doi.org/10.1016/J.WEAR.2009.03.045.